# One- and two-particle microrheology of soft materials based on optical-flow image analysis†

## Electronic Supplementary Information

Matteo Brizioli,[a] Manuel A. Escobedo-Sanchez,[b] Patrick M. McCall,[c] Yael Roichman,[d] Veronique Trappe,[e] Margaret L. Gardel,[c] Stefan U. Egelhaaf,[‡b] Fabio Giavazzi,[*a] and Roberto Cerbino[*f]

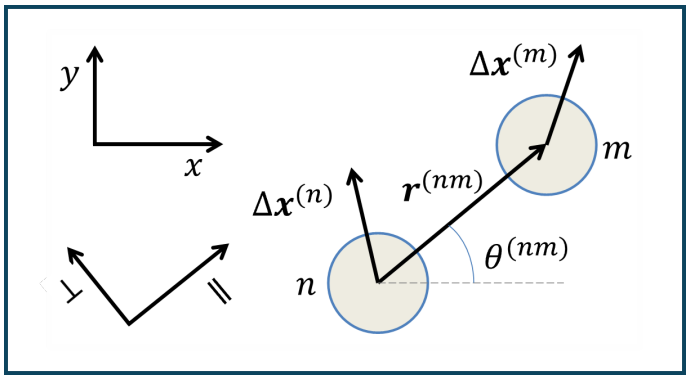


**Fig. S1 Schematic diagram illustrating the decomposition of particle displacements into parallel and perpendicular components**. We consider a pair of particles in the $xy$ plane, labeled $n$ and $m$, respectively. The relative position vector, connecting the center of particle $n$ to the center of particle $m$, is denoted $\mathbf{r}^{(nm)}$. The direction of $\mathbf{r}^{(nm)}$ defines the orientation of the parallel axis $\parallel$, while the orthogonal direction corresponds to the perpendicular axis $\perp$. If $\theta^{(nm)}$ indicates the angle between $\mathbf{r}^{(nm)}$ and the $x$-axis, the parallel (perpendicular) components of the displacement $\Delta\mathbf{x}^{(n)} = (\Delta x_1^{(n)}, \Delta x_2^{(n)})$ reads $\Delta x_\parallel^{(n)} = \Delta x_1^{(n)} \cos\theta^{(nm)} + \Delta x_2^{(n)} \sin\theta^{(nm)}$ ($\Delta x_\perp^{(n)} = -\Delta x_1^{(n)} \sin\theta^{(nm)} + \Delta x_2^{(n)} \cos\theta^{(nm)}$).

[a] *Dipartimento di Biotecnologie Mediche e Medicina Traslazionale, Università degli Studi di Milano, via F.lli Cervi 93, 20090 Segrate, Italy*
*E-mail: fabio.giavazzi@unimi.it*
[b] *Condensed Matter Physics Laboratory, Heinrich Heine University, Universitätsstraße 1, 40225 Düsseldorf, Germany*
[c] *James Franck Institute and Department of Physics, The University of Chicago, Chicago, IL 60637, USA*
[d] *JRaymond & Beverly Sackler School of Chemistry, Tel Aviv University, Tel Aviv 6997801, Israel*
[e] *Department of Physics, University of Fribourg, Chemin du Musée 3, 1700 Fribourg, Switzerland*
[f] *Faculty of Physics, University of Vienna, Boltzmanngasse 5, Vienna 1090, Austria*
*E-mail: roberto.cerbino@univie.ac.at*
[‡] *Deceased.*

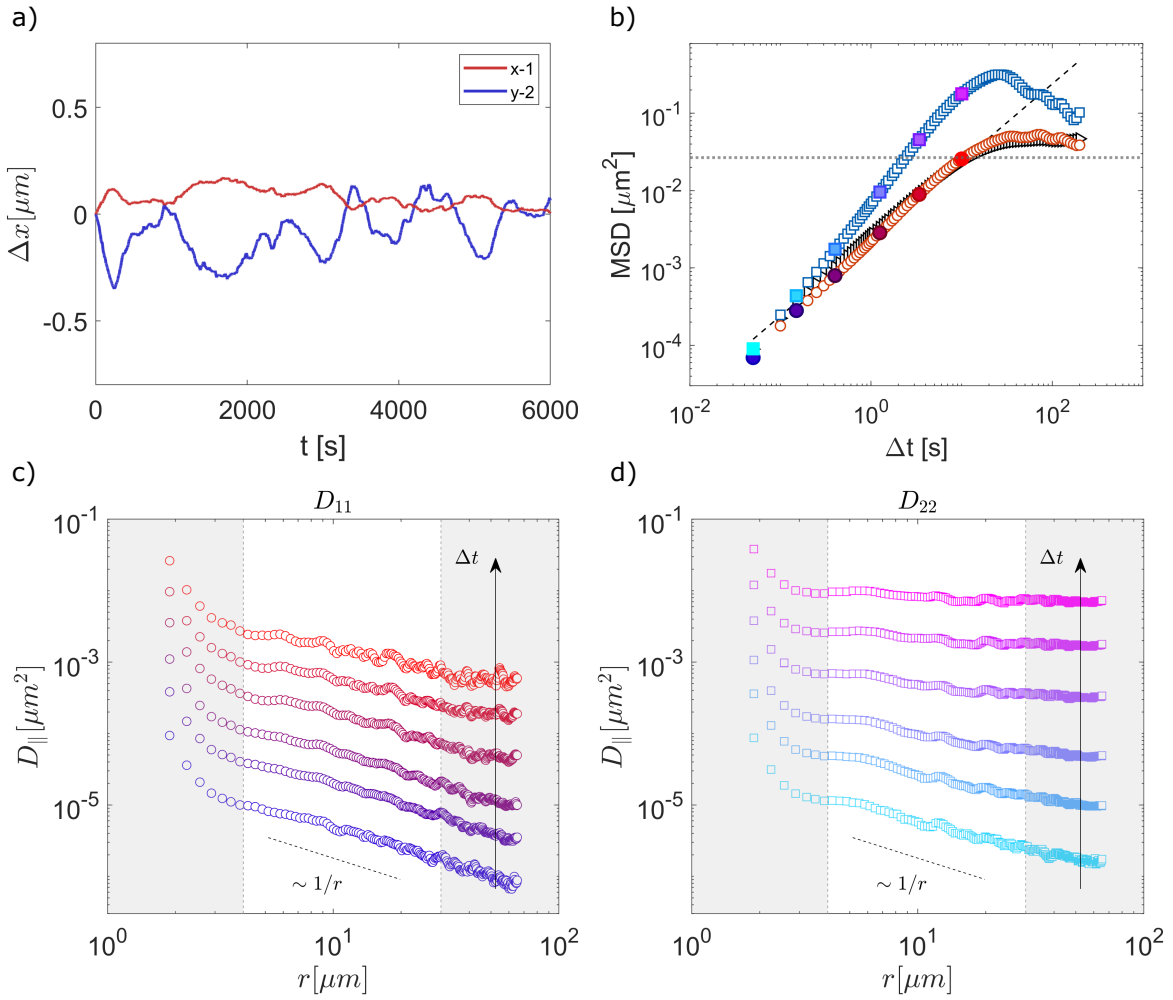


**Fig. S2 Experimental results for a Newtonian Fluid (glycerol-water mixture) in the presence of a mechanical perturbation inducing a shift along the long axis of the capillary ($y$ axis).** (a) Intensity-based image center-of-mass displacement along the $x$ direction (red line) and the $y$ direction (blue line), estimated using the Fiji StackReg plugin. (b) OFM results for one-particle MSD (black triangles) and two-particle MSD computed from $D_{\parallel}$ as estimated from the $D_{11}$ component (red circles) and $D_{22}$ component (blue squares). The two-particle MSD obtained from $D_{22}$ is clearly overestimated due to the global shift in the image. Large symbols correspond to lag-times whose $D_{\parallel}$ obtained from $D_{11}$ and $D_{22}$ are shown in panels (c) and (d), with the same colors. The dashed line corresponds to $2D_0\Delta t$, where $D_0 = (1.20 \pm 0.15) \cdot 10^{-3}$ $\mu m^2/s$ is the diffusion coefficient determined by differential dynamic microscopy. (c,d) $D_{\parallel}$ for different time delays $\Delta t$ in the range [0.05, 10] s as a function of the distance $r$ evaluated from the $D_{11}$ and $D_{22}$ component, respectively. The curves obtained from $D_{22}$ display significant deviations from the expected $\sim 1/r$ scaling for large time delays $\Delta t$.

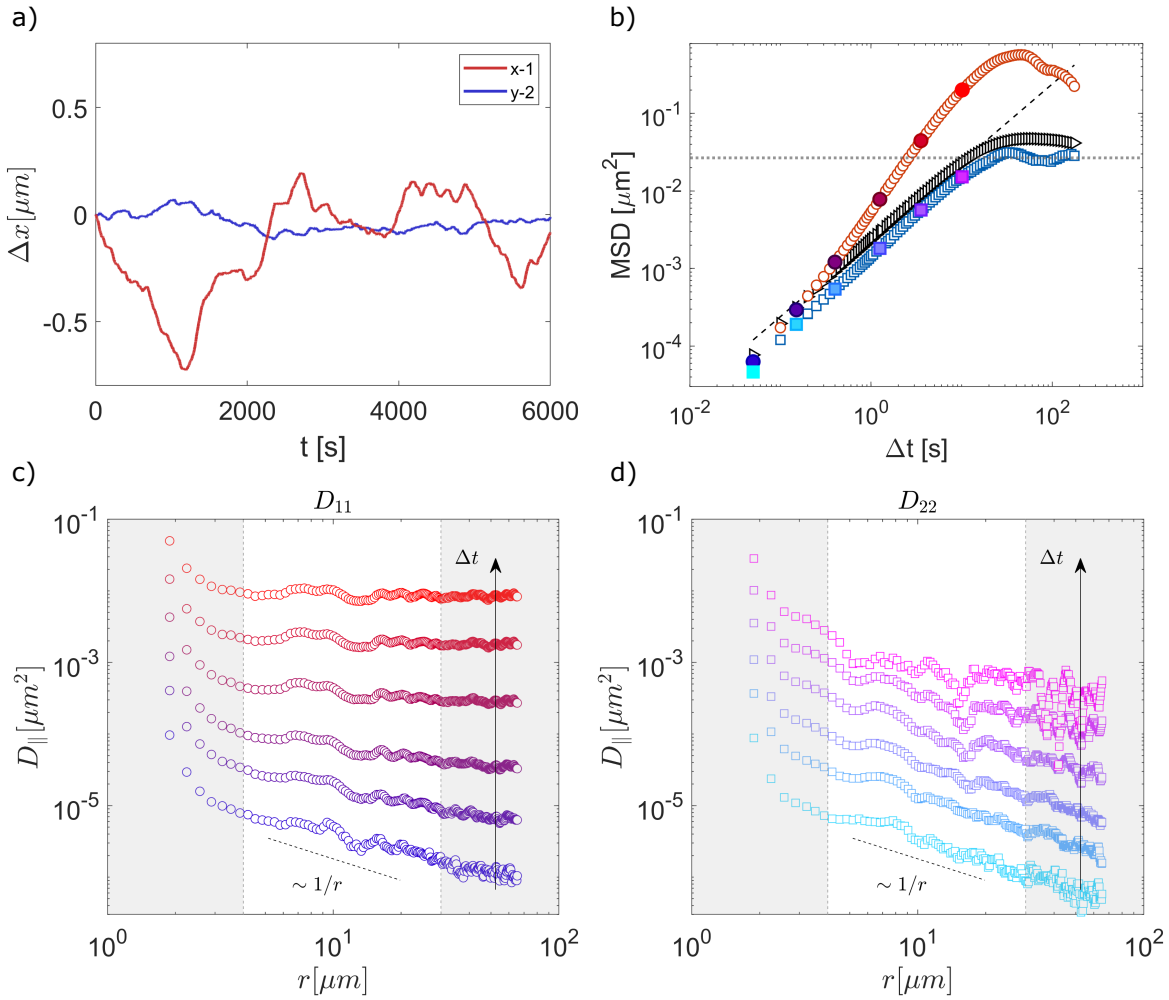


**Fig. S3 Same as in Figure S1, upon a 90° rotation of the capillary**. (a) Intensity-based image center-of-mass displacement along the $x$ direction (red line) and the $y$ direction (blue line), estimated using the Fiji StackReg plugin. (b) OFM results for one-particle MSD (black triangles) and two-particle MSD computed from $D_{\parallel}$ as estimated from the $D_{11}$ component (red circles) and $D_{22}$ component (blue squares). The two-particle MSD obtained from $D_{11}$ is clearly overestimated due to the global shift in the image. Large symbols correspond to lag-times whose $D_{\parallel}$ obtained from $D_{11}$ and $D_{22}$ are shown in panels (c) and (d), with the same colors. The dashed line corresponds to $2D_0\Delta t$, where $D_0 = (1.20 \pm 0.15) \cdot 10^{-3}\ \mu m^2/s$ is the diffusion coefficient determined by differential dynamic microscopy. (c,d) $D_{\parallel}$ for different time delays $\Delta t$ in the range [0.05, 10] s as a function of the distance $r$ evaluated from the $D_{11}$ and $D_{22}$ component, respectively. The curves obtained from $D_{11}$ display significant deviations from the expected $\sim 1/r$ scaling for large time delays $\Delta t$.

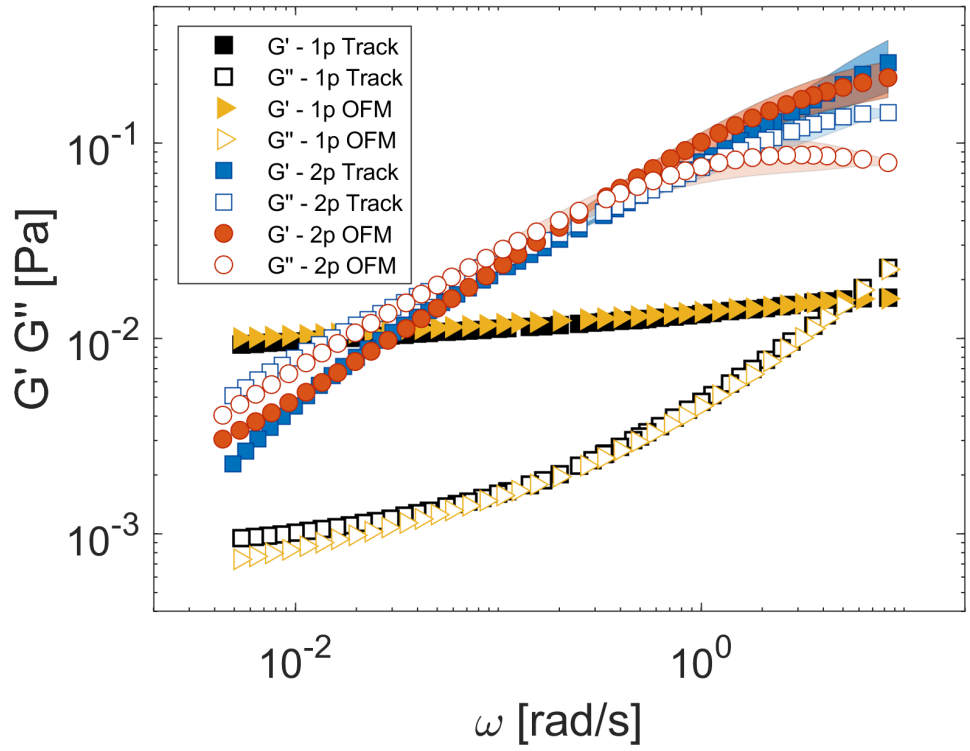


**Fig. S4 Comparison between the elastic modulus $G'(\omega)$ (closed symbols) and loss modulus $G''(\omega)$ for the entangled network of F-actin filaments**. The results are obtained using the one-particle MSD for tracking (black squares) and OFM (yellow triangles) and the two-particle MSD for tracking (blue squares) and OFM (red circles). The evaluation of the moduli from the MSDs has been performed following the methodology presented in Ref.[1].

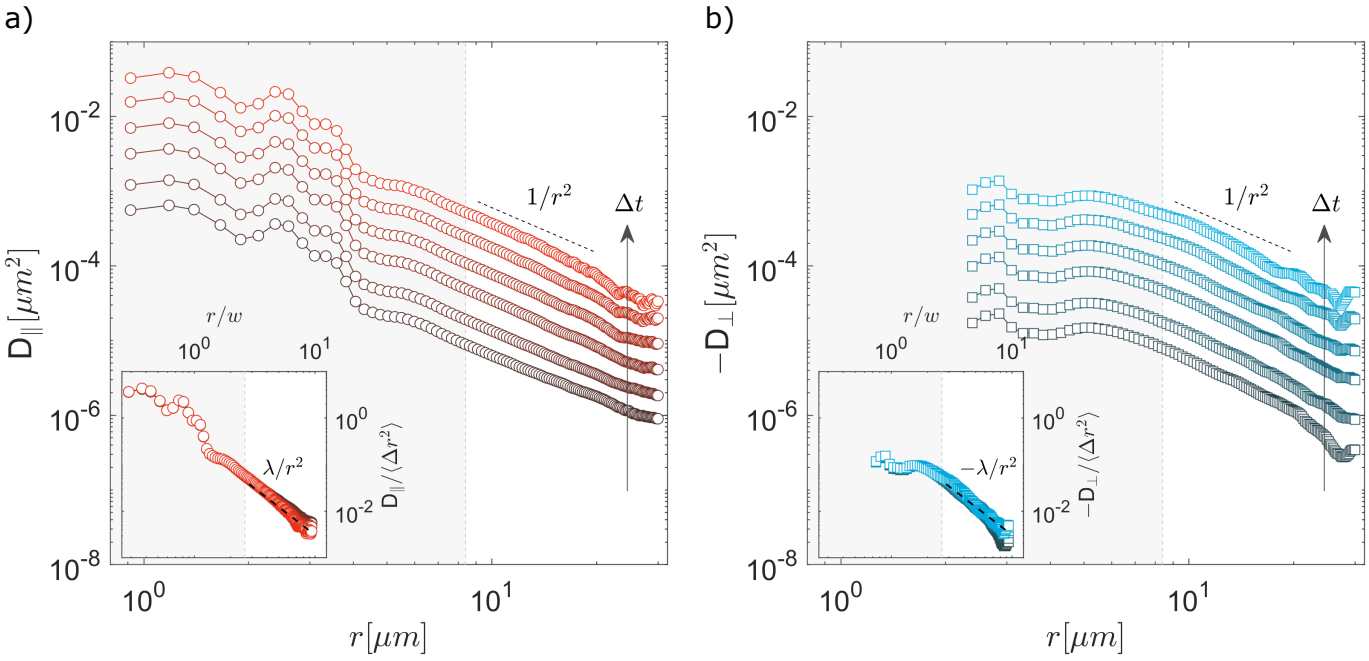


**Fig. S5 Representative displacement cross-correlation tensors at different delay times $\Delta t$ evaluated along the parallel (a) and orthogonal (b) direction for the Quasi-2D colloidal suspension**. Colors varying from dark to bright indicate increasing delay times within the interval $[0.002-0.11]$s. Insets: same data of the main panels normalized by the one-particle MSD $\langle\Delta r^2\rangle$ obtained from OFM (colored symbols) as a function of $r/w$, where $w$ is the cell thickness. Dashed lines correspond to the large-$r$ asymptotic behavior $\pm\lambda(w/r)^2$, where $\lambda=0.31$ is the value reported in Ref.[2] for the same quantities. The white area in each panel denotes the interval $r>3w$, where $D_{\parallel,\perp}$ exhibit $\pm 1/r^2$ scaling.

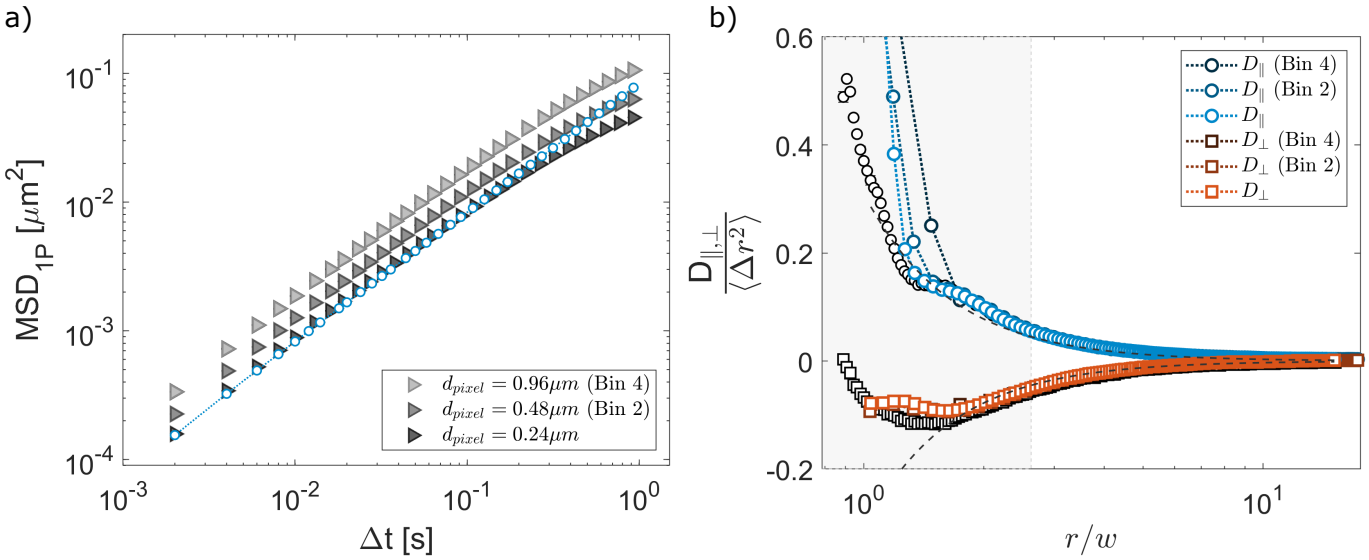


**Fig. S6 Effect of the sampling density on the OFM results for the quasi-2D colloidal suspension.** a) one-particle MSD $\langle\Delta r^2\rangle$ obtained from OFM (triangles) and particle tracking (small circles). The OFM analysis is performed on both the original images (darker symbols) and undersampled copies obtained by binning (2x2 and 4x4, as indicated in the legend) the original images (lighter symbols). Only for the original images the effective pixel size is below the value $\simeq 0.26$ $\mu$m for Nyquist sampling. Larger pixel sizes lead to a systematic overestimate of the one-particle MSD. (b) $D_\|$ (circles) and $D_\perp$ (squares) at time $\Delta t = 0.002$ s normalized by the one-particle MSD $\langle\Delta r^2\rangle$ obtained from OFM (colored symbols) and particle tracking (black and white symbols) as a function of $r/w$, where $w$ is the cell thickness. As in panel (a), results obtained for different effective pixel sizes are represented by symbols with different shades of color, as indicated in the legend. Notably, in the large separation regime $r/w \gg 1$, the normalized cross-correlation tensor provided by OFM analysis is almost insensitive to the effective pixel size.

# Bibliography

1 B. R. Dasgupta, S. Y. Tee, J. C. Crocker, B. J. Frisken and D. A. Weitz, *Physical Review E*, 2002, **65**, 051505.
2 B. Cui, H. Diamant, B. Lin and S. A. Rice, *Physical review letters*, 2004, **92**, 258301.